Title

Maintenance of muscle mass and load-induced growth in Muscle RING Finger 1 null mice with age

Journal

Aging Cell, 13(1)

ISSN

1474-9718

Authors

Hwee, Darren T
Baehr, Leslie M
Philp, Andrew
et al.

Publication Date

2014-02-01

DOI

10.1111/acel.12150

Peer reviewed

Aging Cell (2014) **13**, pp92–101 Doi: 10.1111/acel.12150

Maintenance of muscle mass and load-induced growth in Muscle RING Finger 1 null mice with age

Darren T. Hwee,[1,2] Leslie M. Baehr,[3] Andrew Philp,[1] Keith Baar[1,3] and Sue C. Bodine[1,3]

[1]Departments of Neurobiology, Physiology, and Behavior, [2]Molecular, Cellular and Integrative Physiology Graduate Group, [3]Physiology and Membrane Biology, University of California, Davis, Davis, CA, 95616, USA

Summary

Age-related loss of muscle mass occurs to varying degrees in all individuals and has a detrimental effect on morbidity and mortality. Muscle RING Finger 1 (MuRF1), a muscle-specific E3 ubiquitin ligase, is believed to mediate muscle atrophy through the ubiquitin proteasome system (UPS). Deletion of MuRF1 (KO) in mice attenuates the loss of muscle mass following denervation, disuse, and glucocorticoid treatment; however, its role in age-related muscle loss is unknown. In this study, skeletal muscle from male wild-type (WT) and MuRF1 KO mice was studied up to the age of 24 months. Muscle mass and fiber cross-sectional area decreased significantly with age in WT, but not in KO mice. In aged WT muscle, significant decreases in proteasome activities, especially 20S and 26S β5 (20–40% decrease), were measured and were associated with significant increases in the maladaptive endoplasmic reticulum (ER) stress marker, CHOP. Conversely, in aged MuRF1 KO mice, 20S or 26S β5 proteasome activity was maintained or decreased to a lesser extent than in WT mice, and no increase in CHOP expression was measured. Examination of the growth response of older (18 months) mice to functional overload revealed that old WT mice had significantly less growth relative to young mice (1.37- vs. 1.83-fold), whereas old MuRF1 KO mice had a normal growth response (1.74- vs. 1.90-fold). These data collectively suggest that with age, MuRF1 plays an important role in the control of skeletal muscle mass and growth capacity through the regulation of cellular stress.

Key words: anabolic resistance; ER Stress; sarcopenia; ubiquitin proteasome system.

Introduction

Muscle RING Finger 1, MuRF1, is a muscle-specific E3 ubiquitin ligase that is transcriptionally increased in skeletal muscle in response to a variety of stressors that induce muscle atrophy (Bodine *et al.*, 2001). Deletion of MuRF1 in skeletal muscle has been shown to attenuate the loss of muscle mass under catabolic conditions including denervation, disuse, and glucocorticoid treatment (Labeit *et al.*, 2010; Baehr *et al.*, 2011; Gomes *et al.*, 2012). MuRF1 functions as an E3 ubiquitin ligase, and thus, it has been predicted that muscle sparing in mice with a null deletion of MuRF1 (i.e., MuRF1 KO) would be related to a decrease in proteasome activity. However, a recent study revealed that muscle sparing following denervation is associated with significant increases, not decreases, in both 20S and 26S proteasome subunit activities in MuRF1 KO versus wild-type (WT) mice (Gomes *et al.*, 2012). Furthermore, deletion of MuRF1 was shown to influence Akt/mTOR-mediated signaling and protein synthesis (Baehr *et al.*, 2011; Hwee *et al.*, 2011). Given the muscle-sparing effects of MuRF1 deletion and the possibility that MuRF1 has a role in the regulation of protein quality control, we examined whether mice with a null deletion of MuRF1 demonstrated sparing of muscle mass and load-induced growth as a consequence of aging.

Sarcopenia is the age-related loss of muscle mass and function that occurs to a varying extent in all individuals and can lead to frailty and a decrease in mobility and quality of life (Janssen *et al.*, 2002). A major factor believed to contribute to age-related muscle loss is a change in protein turnover. The ubiquitin proteasome system (UPS) is a tightly regulated system responsible for intracellular protein turnover, including the removal of short-lived normal proteins as well as misfolded and dysfunctional proteins (Koga *et al.*, 2011). The maintenance of proteasome activity and subsequent protein turnover is believed to be necessary for proper cellular function (Wong & Cuervo, 2010). For example, altered proteasome function and the subsequent accumulation of ubiquitin-tagged proteins and protein aggregates have been implicated in the pathology of several neurodegenerative diseases including Parkinson's disease, Alzheimer's disease and Huntington's disease (Vernace *et al.*, 2007; Riederer *et al.*, 2011). Like other cell types, skeletal muscle fibers maintain a continual state of protein renewal through dynamic rates of protein synthesis and degradation. The aging process has been associated with a decrease in proteasome activity in several tissues including brain, liver, and cardiac muscle; however, in skeletal muscle, controversy exists regarding whether proteasome activity is increased, decreased, or unchanged as a function of age (Patterson *et al.*, 2007; Koga *et al.*, 2011; Low, 2011). A number of studies have reported a decrease in proteasome activity in skeletal muscles with advanced age (Lee *et al.*, 1999; Husom *et al.*, 2004; Ferrington *et al.*, 2005; Strucksberg *et al.*, 2010); however, others have reported an age-associated increase in proteasome activity (Hepple *et al.*, 2008; Altun *et al.*, 2010). In the present study, we measured the β1, β2, and β5 20S, and 26S proteasome subunit activities in aged (24 month), but not senescent, WT and MuRF1 KO mice. Given our recent data showing that proteasome activity is enhanced in the MuRF1 KO mice following denervation (Gomes *et al.*, 2012), we hypothesized that with aging, deletion of MuRF1 would result in an elevated level of proteasome activity that would be associated with muscle sparing.

The present study revealed a significant difference in the response of WT and MuRF1 KO mice to aging. Specifically, we found that the growth response to loading was impaired in aged WT mice, but maintained in MuRF1 KO mice. Further, we found that muscle mass and fiber cross-sectional area were maintained in the MuRF1 KO mice with advanced age. A major finding was that both 20S and 26S proteasome activities

Correspondence
Sue C. Bodine, Department of Neurobiology, Physiology, and Behavior, 196 Briggs Hall, University of California, Davis, One Shields Avenue, Davis, CA 95616, USA. Tel.: (530) 752-0694; fax: (530) 752-5582; e-mail: scbodine@ucdavis.edu

Accepted for publication *8 August 2013*

Aging Cell

decreased significantly with age in WT mice. In contrast, the activities of the majority of the proteasome subunits in the old MuRF1 KO mice were significantly higher than the activities measured in the old WT mice. Overall, the data suggest that deletion of MuRF1 maintains protein quality control in skeletal muscle, leading to reductions in endoplasmic reticulum and oxidative stress and the maintenance of muscle mass and growth capacity.

Results

MuRF1 deletion spares muscle mass and fiber cross-sectional area and increases capillary density with age

Given that muscle mass is spared in MuRF1 KO mice following denervation and other atrophy-inducing conditions, we examined whether MuRF1 KO mice were resistant to age-related muscle loss. Skeletal muscle mass, fiber cross-sectional area, and maximum isometric force were similar in WT and MuRF1 KO mice up to the age of 18 months (Fig. 1, Table 1). At 24 months of age, significant muscle atrophy occurred in WT mice as measured by a decrease in muscle mass, fiber area, and maximum isometric tension (Fig. 1, Table 1). In contrast, 24-month-old KO mice had no decrease in muscle mass or fiber cross-sectional area relative to young adult KO mice. Unexpectedly, maximum isometric tension was significantly down in the 24-month-old KO mice even though there was significant sparing of muscle mass. Moreover, the age-associated decrease in tension output was greater in the KO than the WT mice (Fig. S1). Given that tension was measured via direct nerve stimulation, the drop in tension output may reflect denervation or a decrease in synaptic efficacy. Analysis of the isometric twitch revealed a slowing of both time-to-peak tension and half relaxation time in both WT and KO mice (Table S1).

Another characteristic of aging muscle that was examined in WT and KO mice was capillary density. Capillary density was not significantly different in WT and KO mice at 18 m or younger; however, at 24 m, capillary density significantly increased in the MuRF1 KO mice resulting in a significant difference between KO and WT mice (Fig. 2A, Fig. S2). Interestingly, expression of HIF-1α protein was significantly higher in KO than WT mice at both 9 and 24 months. Moreover, there was a significant increase in HIF-1α expression in KO mice between 9 and 24 months (Fig. 2B).

MAFbx expression is elevated in MuRF1 KO, but not in WT mice with aging

The expression of select genes associated with denervation and aging was assessed in young (6 m) and old (24 m) WT and KO mice (Fig. 2C). No significant changes were observed for FOXO1 or MuRF1 expression with age. Embryonic myosin heavy chain, a gene associated with inactivity and regeneration, was elevated significantly in both old WT and KO mice. MAFbx, a muscle-specific E3 ligase associated with denervation and atrophy, significantly increased with age in the KO, but not in WT mice. Expression of CHIP, an ubiquitin ligase that promotes the degradation of unfolded proteins, was slightly elevated in old KO ($P = 0.06$), but not in WT ($P = 0.11$) mice.

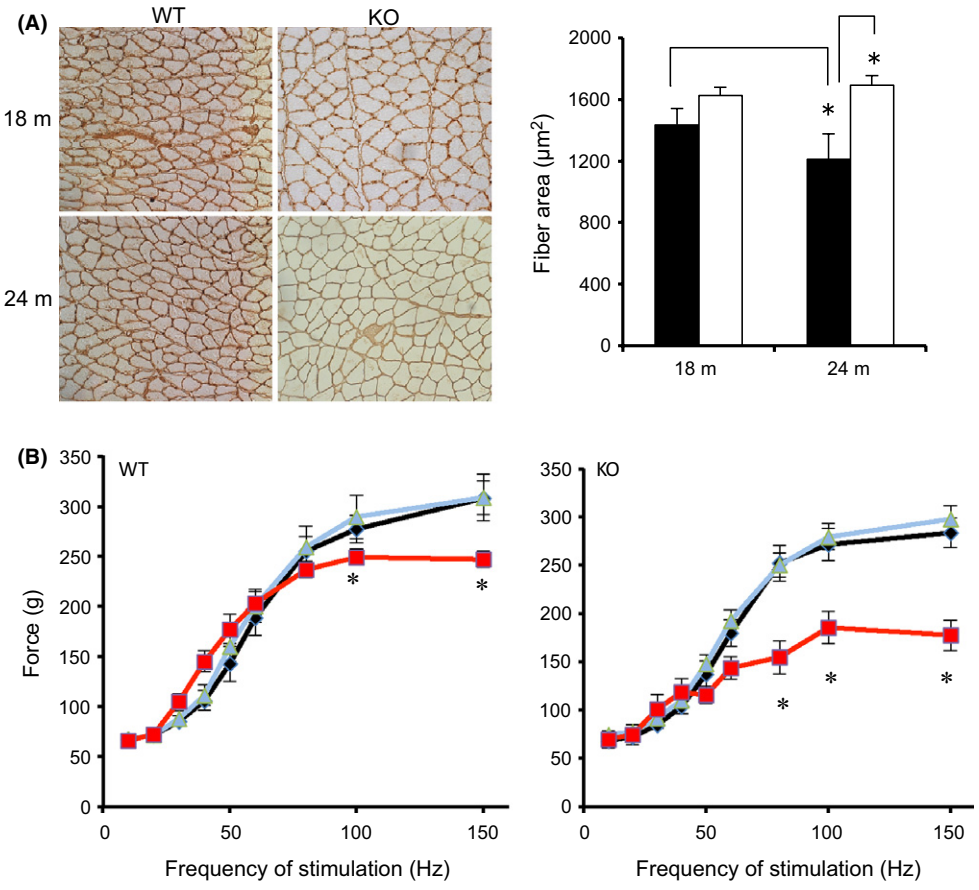

Fig. 1 Maintenance of muscle mass in MuRF1 KO mice with aging. (A) Representative laminin-stained sections from 18- and 24-month-old WT and MuRF1 KO mice. (B) Average fiber cross-sectional area of the gastrocnemius muscle (medial and lateral heads) of WT (black) and MuRF1 KO (white) at 18 and 24 months. (C) *In situ* isometric contractile force measurements of the gastrocnemius muscle of WT and MuRF1 KO mice at 8 (black), 18 (blue), and 24 (red) months of age. Data are mean ± SEM, n ≥ 5 mice per group. Statistical significance was set at $P < 0.05$ and determine using a two-way ANOVA for CSA and one-way ANOVA for force output. * indicates significant differences between groups identified by the brackets (A) or between ages for a specific frequency of stimulation (B).

Table 1 Body weight and muscle mass of WT and MuRF1 KO animals

	BW (g)	Heart (g)	TA (g)	GA complex (g)
6 m WT	31.9 ± 1.8	0.144 ± 0.006	0.054 ± 0.002	0.183 ± 0.007
6 m KO	35.7 ± 2.1	0.175 ± 0.005*	0.056 ± 0.002	0.193 ± 0.004
12 m WT	35.4 ± 1.4	0.158 ± 0.004	0.058 ± 0.001	0.192 ± 0.003
12 m KO	32.0 ± 1.1	0.210 ± 0.003*	0.056 ± 0.001	0.199 ± 0.003
18 m WT	36.7 ± 3.7	0.168 ± 0.007		0.173 ± 0.003
18 m KO	36.2 ± 2.0	0.208 ± 0.004		0.181 ± 0.005
24 m WT	36.4 ± 0.8	0.179 ± 0.005	0.051 ± 0.002	0.159 ± 0.006#
24 m KO	39.1 ± 1.3	0.247 ± 0.008*	0.055 ± 0.001	0.184 ± 0.004*

Body weight (BW), heart, and hindlimb skeletal muscle (tibialis anterior (TA), gastrocnemius (GA) complex (medial and lateral gastrocnemius, soleus, and plantaris) masses (wet weight) from WT and MuRF1 KO male mice at 6, 12, 18, and 24 months of age. Values are expressed as mean ± SEM. A two-way ANOVA was performed with Tukey's post hoc analysis. Statistical significance was set at $P < 0.05$.

*indicates significant difference between WT and KO mice at a specific age;

#indicates significance difference between 6 and 24 month old mice of a specific genotype.

The ubiquitin proteasome system is maintained in aged MuRF1 KO mice

Accumulation of ubiquitinated and damaged proteins occurs in muscle with aging and has been associated with a decrease in the UPS (Combaret *et al.*, 2009). Here, we found that polyubiquitinated proteins increased significantly in both WT and KO muscles as a function of age, as assessed by Western blot and ELISA (Fig. 3). Next, we measured the ATP-dependent (26S) and ATP-independent (20S) activities of the catalytic subunits (β1, β2, β5) in the gastrocnemius muscle of young (6 m) and old (24 m) WT and KO mice (Fig. 3C). In WT mice, the activities of all 20S and 26S catalytic subunits, except for the 26S β2, significantly decreased with age, accounting for the observed accumulation of polyubiquitinated proteins. For the majority of subunits (4 of 6), proteolytic activity was significantly higher in the old KO than WT mice.

To determine whether the change in proteasome subunit activity was related to alterations in the amount of proteasome, Western blots were performed for specific 19S (RPT6, RPT1) and 20S (β5, PSMA6) proteasome subunits. No age-related changes were observed for any of the subunits in WT or KO mice (Fig. S3). Measurement of the inducible subunits β1i and β5i did reveal age-related changes in both WT and KO mice. A significant increase in β1i expression was measured in both WT and KO mice with age, while β5i expression significantly increased only in WT mice with age. (Fig. S3). Expression of PA28α was greater in KO than WT adult mice (9 m); however, PA28α expression was similar in old (24 m) WT and KO mice due to a significant increase in expression in the WT mice from 9 to 24 months of age (Fig. S3).

Oxidative and ER Stress are differentially regulated in WT and MuRF1 KO mice with age

To determine whether there was an increase in oxidative stress with age, the level of oxidatively modified proteins was measured in the gastrocnemius of young and old WT and KO mice (Fig. 4A). In young mice, the amount of oxidized proteins was significantly lower in MuRF1 KO than WT mice. With age, however, the level of oxidized proteins significantly increased in the KO, but not in WT mice. Increases in oxidative stress have been associated with increases in calpain and

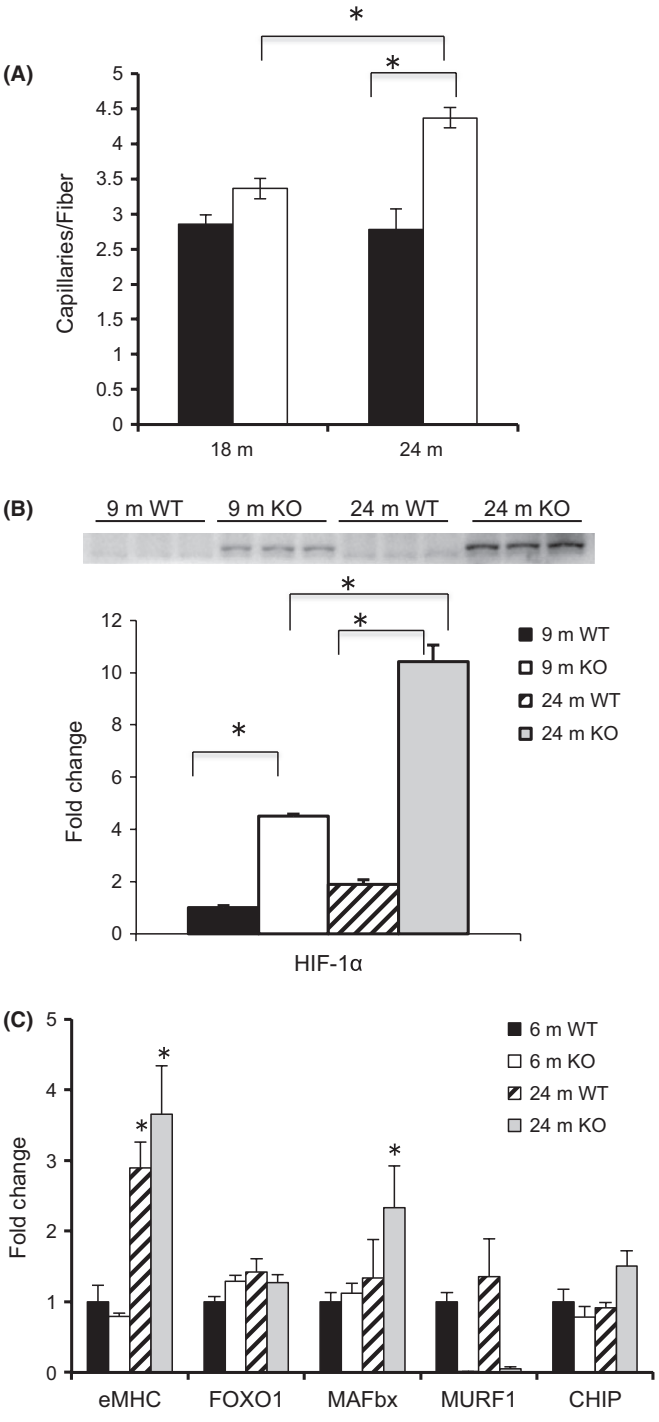

Fig. 2 Capillary density and differential gene expression in WT and MuRF1 KO mice with age. (A) Capillary density, measured as the number of capillaries per muscle fiber, was determined in the medial and lateral gastrocnemius muscle from CD31 stained cross sections in 18- and 24-month-old WT (black) and KO (white) mice. (B) Representative Western blot of HIF-1α from homogenates of the gastrocnemius complex taken from young adult (9 m) and old (24 m) WT and MuRF1 KO mice. Means ± SEM ($n = 4$ per group) are expressed as a fold change relative to the 9 m WT mean. (C) The mRNA expression levels of selected genes were determined from homogenates of the gastrocnemius complex of young (6 m) and old (24 m) WT and MuRF1 KO mice. Means (±SEM, $n \geq 4$ per group) are expressed as a fold change relative to the 6 m WT mean. Statistical significance was set at $P < 0.05$ and determined using a two-way ANOVA. * indicates significant differences between groups identified by the brackets.

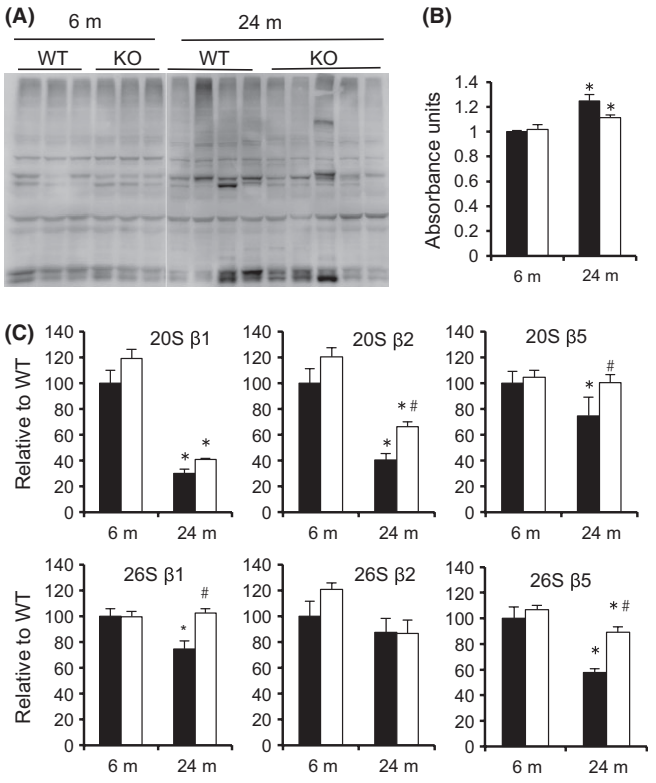

Fig. 3 Higher levels of proteasome activity in MuRF1 KO mice relative to WT with aging. (A) Western blots of lysates from the gastrocnemius complex of young (6 m, $n = 3$) and old (24 m, $n = 4$) WT and MuRF1 KO mice. Polyubiquitinated proteins were determined by immunoblotting with an anti-ubiquitin antibody (FK1). (B) Polyubiquitin levels were quantified by ELISA in 6-m and 24-m-old wild-type (black) and MuRF1 KO (white). Data are mean ± SEM for $n = 4$–5 per group. (C) ATP-dependent (26S) and ATP-independent (20S) proteasome activities in lysates from the gastrocnemius complex of WT (black) and MuRF1 KO (white) mice at 6 and 24 months. Individual subunit activities are shown for β1, caspase-like activity; β2, trypsin-like activity; and β5, chymotrypsin-like activity. Data are mean ± SEM, $n = 4$ mice per group. Statistical significance was set at $P < 0.05$ and determined using a two-way ANOVA. *indicates significant difference between young and old within a specific genotype, #indicates significant difference between WT and KO mice at a given age. * indicates significant differences between groups identified by the brackets.

caspase-3 activities, which were subsequently measured in young and old mice (Fig. 4B,C) (Whidden *et al.*, 2010; Nelson *et al.*, 2012). Calpain (I and II) activity was similar in WT and KO mice at 6 m and significantly decreased in both WT and KO mice at 24 m. In contrast, caspase-3 activity was similar in WT and KO mice at 6 m, but significantly increased at 24 m in the KO mice only. Interestingly, levels of the anti-apoptosis protein, Bcl-2, were significantly higher in the KO mice at 24 m (Fig. 4D).

Endoplasmic reticulum (ER) stress, as measured by BiP, PDI, and CHOP expression, was also examined as a function of age in the WT and KO mice (Fig. 5). Both of the adaptive stress markers, BiP and PDI, increased significantly as a function of age (6 m vs. 24 m) in WT and KO mice. In contrast, the maladaptive marker, CHOP, increased significantly at 24 m in WT, but not in KO, mice.

The growth response to functional overload is blunted in aging WT, but not in MuRF1 KO mice

Aging not only results in a loss of muscle mass, but also results in anabolic resistance, that is, the inability to respond to growth cues. The growth response of skeletal muscle to increased mechanical loading is attenuated in aging rodents as early as 18 month of age (Hwee & Bodine, 2009). Thus, we examined the growth response of the plantaris muscle from young (6 m) and older (18–20 m) WT and MuRF1 KO mice to increase mechanical loading using the functional overload (FO) model. At 18 month of age, WT and KO mice had similar muscle mass and demonstrated no age-related muscle loss (Table 1). Following 14 days of overload, growth of the plantaris was similar in young WT and KO mice (Fig. 6A). In contrast, older WT mice showed a significant decrease in the amount of growth relative to young mice (1.37- vs 1.83-fold), while older KO mice had a growth response that was similar to the young mice (1.74- vs. 1.90-fold). To further examine the dynamics of the growth response, we measured the response of older WT and KO mice to 7 and 14 days of overload. These experiments revealed that during the first 7 days of overload, muscle growth was similar in old WT and KO mice; however, between 7 and 14 days, muscle growth plateaued in the WT mice, while muscle growth continued in the KO mice (Fig. 6B).

Previous publications have shown that with age, activation of the Akt/mTOR signaling pathway is blunted leading to attenuated muscle hypertrophy in response to mechanical load (Thomson & Gordon, 2006; Hwee & Bodine, 2009). In this study, we found that after 7 days of overload, activation of both PKB/Akt and S6K1 was significantly higher in KO compared with WT mice (Fig. 6C, Fig. S4).

In skeletal muscle, ER stress mediates anabolic resistance through PKB/Akt inhibition (Deldicque *et al.*, 2011). The accumulation of unfolded or misfolded proteins in the ER can occur during periods of high rates of synthesis, as occur during functional overload (Zhang & Kaufman, 2006). Examination of the expression of the adaptive and maladaptive ER stress markers revealed a significant increase in ER stress in response to overload in both WT and KO mice (Fig. 6D,E). Of particular interest was the finding that the maladaptive ER stress response, as denoted by CHOP levels, increased to a greater extent in both young and old WT compared with KO mice following overload.

Discussion

Muscle RING Finger 1 (MuRF1), a muscle-specific E3 ubiquitin ligase, is an atrophy-associated gene that is transcriptionally increased following denervation and disuse, two processes associated with aging (Bodine *et al.*, 2001). The extent to which MuRF1 is involved in the aging process is controversial because both no change (Leger *et al.*, 2008; Gaugler *et al.*, 2011) and increased (Clavel *et al.*, 2006) expression of MuRF1 have been reported in aging muscle. A key finding in this study was that the activities of both the 20S and 26S proteasomal subunits decreased significantly with age in WT mice, but were maintained or decreased to a lesser extent in the MuRF1 KO mice with age. Further, we demonstrate that the absence of MuRF1 results in the maintenance of two properties shown to decrease with age, that is, muscle mass and skeletal muscle growth in response to increased loading, which suggests that MuRF1 expression plays an important role in the regulation of skeletal muscle mass and function with age. These data are contrary to prevailing theory that age-related loss of muscle mass is caused by an increase in the ubiquitin proteasome system (Altun *et al.*, 2010). Instead, these data suggest that a decrease, in proteasome activity with aging contributes to cellular dysfunction in skeletal muscle, as indicated by an increase in ER stress. The current findings support the theory that maintaining or increasing protein turnover decreases

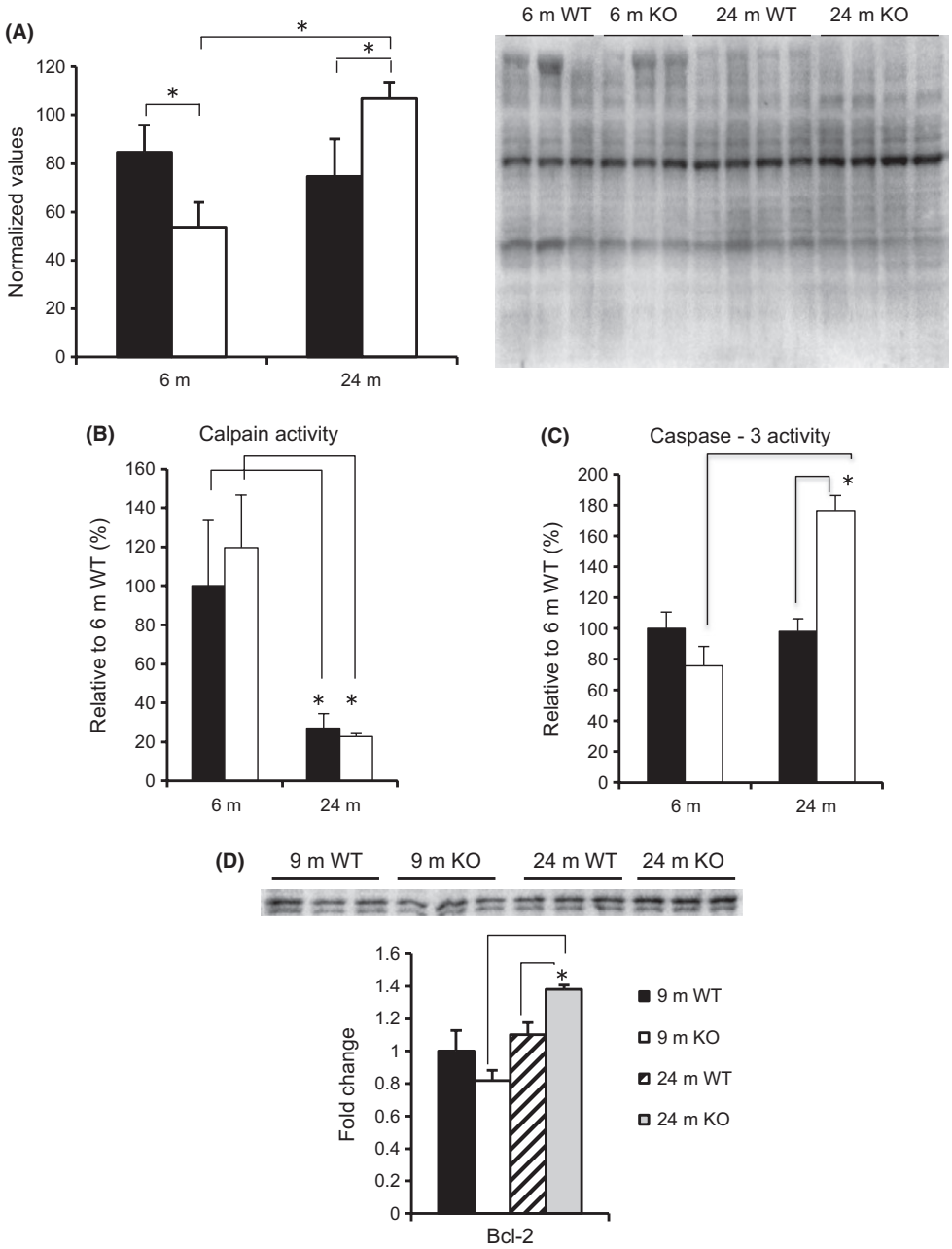

Fig. 4 Oxidative stress in WT and KO mice. (A) Oxidized proteins were measured in the gastrocnemius muscle of young (6 m) and old (24 m) WT (black) and KO (white) mice using the OxiSelect™ Protein Carbonyl Immunoblot Kit. Data are mean ± SEM, n = 3–4 mice. Calpain (B) and caspase-3 (C) activities were measured in the gastrocnemius of WT (black) and KO (white) mice. Means ± SEM are expressed as a percent of 6 m WT mean. (D) Western blot of Bcl-2 from homogenates of the gastrocnemius taken from young adult (9 m) and old (24 m) WT and MuRF1 KO mice. Means ± SEM (n = 3 per group) are expressed as a fold change relative to the 6 m WT mean. Statistical significance was set at $P < 0.05$ and determined using a two-way ANOVA. * indicates significant differences between groups identified by the brackets.

cellular dysfunction and is beneficial to maintaining muscle mass during aging.

The ubiquitin proteasome system and age-related muscle loss

The UPS is responsible for the removal of short-lived, dysfunctional, and misfolded proteins (Koga *et al.*, 2011). Its role in protein turnover is critical for optimal cell performance, as a decrease in proteasome activity has been shown to lead to an accumulation of protein aggregates and overall cellular dysfunction (Wong & Cuervo, 2010). Increases in UPS activity are implicated in a number of conditions that induce skeletal muscle atrophy and are believed to play a role in age-related muscle loss (Combaret *et al.*, 2009). Aging is a slow progressive process that leads to decreases in skeletal muscle mass and strength, contributing to increases in morbidity and mortality. Although it is generally accepted in other tissues that the UPS decreases with aging, its activity in skeletal muscle with aging is less clear, as both increases (Hepple *et al.*, 2008; Altun *et al.*, 2010) and decreases (Husom *et al.*, 2004; Ferrington *et al.*, 2005; Strucksberg *et al.*, 2010) in proteasome activity have been reported in aging muscle. The present study measured the 20S and 26S proteasome activities of all three (β1, β2, and β5) subunits in old mice (24 months) on a C57Bl6 background and found a significant decrease in the activity in 5 of 6 of the subunits. In MuRF1 KO mice, the activity of 4 of these subunits and overall β5 activity was higher in the KO mice than the WT. The higher proteasome activities in the aged MuRF1 KO versus WT mice could be playing a role in the observed maintenance of muscle mass and fiber cross-sectional area with age. Recently, we reported that muscle sparing in the MuRF1 KO mice following denervation was associated with an increase, not a decrease, in

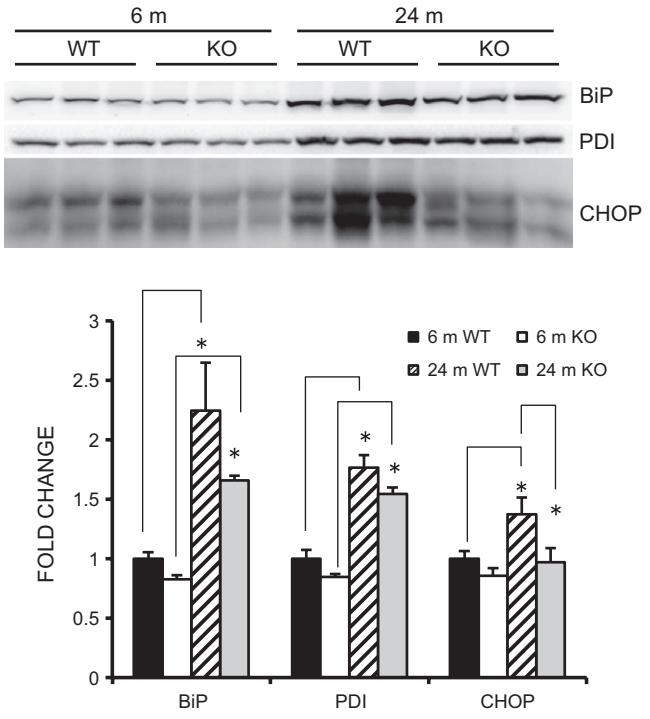

Fig. 5 Markers of endoplasmic reticulum (ER) stress are elevated in old WT, but not in MuRF1 KO mice. Representative Western blots of ER stress markers (BiP, PDI, and CHOP) from homogenates of the gastrocnemius taken from young adult (6 m) and old (24 m) WT and MuRF1 KO mice. Means ± SEM (n = 4 per group) are expressed as a fold change relative to the 6 m WT mean. Statistical significance was set at $P < 0.05$ and determined using a two-way ANOVA. * indicates significant differences between groups identified by the brackets.

proteasome activity relative to WT mice (Gomes *et al.*, 2012). The idea that elevated proteasome activity is beneficial for cellular function is not new, and several recent studies have shown that impairment of proteasome activity is harmful to muscle (Anvar *et al.*, 2011). Recently, a transgenic mouse was developed with decreased proteasome chymotrypsin-like (β5) activity and showed a shortened lifespan and a decrease in muscle mass (Haas *et al.*, 2007; Tomaru *et al.*, 2012). Mice with a deletion of carboxyl terminus of HSP70-interacting protein (CHIP) also demonstrate a shortened lifespan and accelerated loss of skeletal muscle mass, and coincidentally have defects in protein quality control and an accelerated loss of chymotrypsin-like (β5) activity with age (Min *et al.*, 2008). Interestingly, we observed an increase in the expression of CHIP, as well as MAFbx, in the aged KO mice.

The mechanism responsible for the elevated proteasome activity in the old MuRF1 KO is unknown. One factor that could be contributing to the lack of inactivation of proteasome activity in the MuRF1 KO mice with age is the increased MAFbx expression. In a previous study, we noted that in response to neural inactivity, the absence of MuRF1 results in sustained elevated levels of MAFbx expression, suggesting that MuRF1 is involved in a feedback loop that controls MAFbx expression (Gomes *et al.*, 2012). Of relevance to the current study was the finding that following denervation, proteasome activity was higher in the MuRF1 KO compared with WT mice. It is possible that the elevated proteasome activity in the old MuRF1 KO mice is linked to neural inactivity. The mechanism by which MuRF1 deletion spares muscle mass under conditions of inactivity may be related to an increased ability to decrease cellular stress and maintain global protein synthesis.

The reciprocal UPS and ER Stress Relationship

One potential consequence of diminished proteasome capacity is the accumulation of misfolded or dysfunctional proteins that compromise endoplasmic reticulum-associated protein degradation (ERAD). The accumulation of misfolded or unfolded proteins in the endoplasmic reticulum can lead to ER stress and the unfolded protein response (Fu *et al.*, 2008). The initial ER stress response is adaptive yielding an increase in the protein folding capacity of the cell and a decrease in protein translation. When the unfolded protein response fails, however, cells may initiate a maladaptive response, that is, apoptosis. We found that aged WT muscle had increased BiP, a chaperone protein indicative of the adaptive ER stress response, and CHOP, a pro-apoptotic marker of the maladaptive ER stress response. In contrast, in old MuRF1 KO muscle, BiP levels were high in the absence of changes in CHOP levels. Interestingly, we found an increase in caspase-3 activity in the old KO mice. Classically, caspase-3 has been used as an indicator of increases in apoptosis. However, in muscle, the elevated caspase-3 could be involved in an increase in myofilament turnover (Du *et al.*, 2004) and proteasome activation (Wang *et al.*, 2010), which is consistent with the elevated proteasome activity seen in the MuRF1 KO mice. Our observed increase in the anti-apoptosis marker Bcl-2 in the MuRF1 KO mice with age could suggest a mechanism to protect the muscle from the apoptotic affects of increased caspase-3.

Overall, the data suggest that deletion of MuRF1 results in reduced levels of cellular stress. In young mice, the amount of oxidized proteins was significantly lower in MuRF1 KO mice than that in WT mice. With age, ER stress increased in the WT mice without an apparent increase in the amount of oxidized proteins. In contrast, the amount of oxidized proteins significantly increased in the MuRF1 KO mice with age, without an increase in the maladaptive ER stress response but an increase in the adaptive ER stress response. The elevated oxidative stress in the MuRF1 KO mice could be the result of denervation (discussed below); however, it appears that the MuRF1 KO mice are capable of increasing anti-oxidant defenses that protect the muscle from atrophy. Increases in HIF-1α, caspase-3, and Bcl-2 expression, and proteasome activity in the old MuRF1 KO mice could all be playing a role in reducing ER stress and protecting the muscle from atrophy.

MuRF1 expression and age-associated loss of muscle mass

The loss of MuRF1 expression results in muscle sparing under a number of atrophy-inducing condition, including denervation (Baehr *et al.*, 2011; Gomes *et al.*, 2012). The present results reveal that the deletion of MuRF1 also has a positive impact on the aging process resulting in the sparing of muscle mass and the retention of the growth response. Aging is associated with anabolic resistance, that is, the loss of the ability to increase muscle mass in response to anabolic signals such as increased loading, which is attributed to a decrease in the activation of mTORC1-mediated signaling and protein translation. The retention of the load-induced growth response in the MuRF1 KO mice was associated with less ER stress and greater activation of PKB/Akt and S6K1, a downstream target of mTORC1, relative to WT mice and suggests that there was greater activation of protein translation in the old MuRF1 KO compared with WT mice. The attenuation of load-induced growth occurs with aging (Hwee & Bodine, 2009) and diet-induced obesity (Sitnick *et al.*, 2009) and is related to a decrease or delay in the activation of Akt and mTORC1 signaling. In mice, S6K1 activation peaks at around 7 days following functional overload in young mice; however, in the present study, we observed a reduced and delayed activation of S6K1 in the old

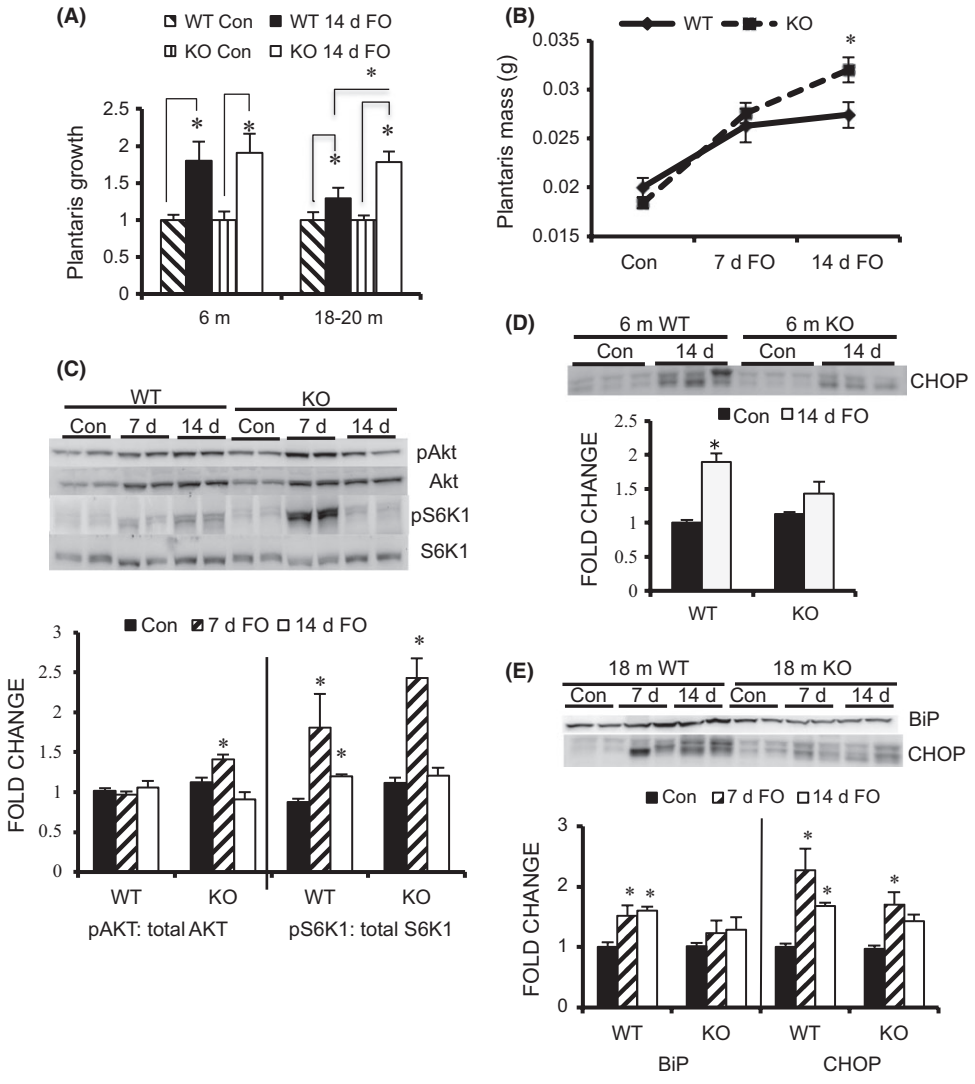

Fig. 6 Load-induced growth is maintained in older MuRF1 KO mice compared with WT mice. (A) Growth of the plantaris muscle (fold change relative to control, mean ± SEM, $n = 5$) following 14 days of functional overload (FO) in young (6 m) and older (18–20 m) WT (black) and MuRF1 KO (white) mice. (B) Growth of the plantaris muscle (wet weight in grams) following 7 and 14 days of FO in 18- to 20-month-old WT (solid) and MuRF1 KO (dashed) mice. (C) Representative Western blots ($n = 2$) and quantification ($n = 4$) of the phosphorylation levels of Akt and S6K1 in the plantaris muscle of old (18–20 m) WT and KO mice following no treatment (Con, black) and FO for 7 (hatched) and 14 (white) days. (D) Representative Western blot ($n = 3$) and quantification ($n = 5$) of CHOP protein levels in the plantaris of young WT and MuRF1 KO mice following no treatment (Con, black) and 14 days of FO (white). (E) Representative Western blot ($n = 2$) and quantification ($n = 4$) of BiP and CHOP protein levels in the plantaris of older (18 m) WT and MuRF1 KO mice following no treatment (Con, black) and FO for 7 (hatched) and 14 days (white). Data are expressed as a fold change relative to WT control (mean ± SEM). Statistical significance was set at $P < 0.05$ and determined using a two-way ANOVA for growth and a one-way ANOVA for protein expression. * indicates significant differences between groups identified by the brackets.

WT mice and normal activation of S6K1 in the old MuRF1 KO mice. The pattern of Akt and S6K1 activation observed in the old WT mice following FO is consistent with previous observations in old rats and DIO mice, which have a reduced load-induced growth response (Hwee & Bodine, 2009; Sitnick *et al.*, 2009). Our data suggest that deletion of MuRF1 leads to less cellular stress and the ability to maintain a net positive protein balance in aged animals in response to increased loading. Previous data have demonstrated that elevated ER stress can inhibit the Akt/mTORC1 signaling and protein translation in skeletal muscle (Deldicque *et al.*, 2011). Additional experiments are required to directly test the hypothesis that the ability to induce a normal growth response in muscle from old MuRF1 KO mice is related to a reduced level of ER stress, leading to greater activation of protein translation.

MuRF1 and the neuromuscular junction

One perplexing finding is the fact that muscle force output, as measured *in situ* through stimulation of the nerve, was significantly less in the old MuRF1 KO mice relative to the old WT mice. At 18 months of age, the maximum isometric force output of the WT and KO mice is similar; however, by 24 months, force output is diminished in both the WT and KO mice with a greater decrease in the KO than WT mice. These data might suggest a greater loss of myofilament proteins in the KO relative to the WT mice; however, the fiber CSA was higher in the MuRF1 animals, and the relative amount of myosin heavy chain and actin was similar in the old MuRF1 and WT KO mice (data not shown). Another explanation could be that there is more denervation or synaptic instability in the old MuRF1 KO mice compared with the WT mice. Synaptic remodeling occurs as early as 18 months of age in C57BL6 mice as neuromuscular junctions begin to lose innervation and either become reinnervated or remain denervated (Valdez *et al.*, 2010). We have observed that following denervation in the MuRF1 KO mice, there is a decrease in expression of myogenin and acetylcholine receptor subunits (manuscript in submission). The suppression of various activity-associated genes could stabilize the neuromuscular junction and inhibit reinnervation in the MuRF1 KO mice during this time of motoneuron loss and synapse remodeling. Interestingly, a recent paper reports that MuRF1 controls the turnover of the acetylcholine receptor (AChR) (Rudolf *et al.*, 2012). Under normal fully innervated conditions, no difference was found in the turnover of the AChR in WT and MuRF1 KO mice; however, following denervation, turnover of the AChR was significantly higher in the WT compared with the KO mice. Our observations in aging MuRF1 KO mice suggest that a lack of synaptic

remodeling may suppress reinnervation resulting in chronically denervated muscle fibers; however, this theory requires further investigation.

In conclusion, the deletion of the MuRF1 gene and protein expression is beneficial to muscle during aging. The mechanism of action appears to be through the maintenance of protein quality control and suppression of cellular stress. These data highlight the need for additional efforts to identify the *in vivo* substrates of MuRF1 in skeletal muscle and to determine the mechanism by which MuRF1 functions to reduce cellular stress and maintain muscle mass and growth capacity.

Experimental procedures

Animals

The generation of mice with a null deletion of MuRF1 has been previously described (Bodine *et al.*, 2001). Homozygous knockout (KO) and wild-type (WT) mice were obtained by intercrossing heterozygous MuRF1 mice. A total of 78 male mice, ranging in age from 6 to 24 months, were used in this study. Mice were kept under a 12-h light–dark cycle and were fed standard diets. The Institutional Animal Care and Use Committee at the University of California, Davis, approved all animal protocols used in this study.

Functional overload model

The plantaris muscle in both legs was overloaded by the surgical removal of its major synergists: the soleus and medial and lateral gastrocnemius muscles. Animals were anesthetized with isoflurane gas and prepared for surgery using aseptic procedures. Mice were given buprenorphine postsurgery for pain and monitored on a daily basis until the muscles were removed 7–14 days postsurgery.

Histology

The gastrocnemius complex (soleus, medial and lateral gastrocnemius, plantaris) was excised, cleaned, pinned to corkboard, and frozen in melting isopentane. Serial cross sections (10 μm) were stained with hematoxylin and eosin for the evaluation of general histology, antilaminin (1:1000, Sigma, St. Louis, MO, USA) for the measurement of fiber cross-sectional area, and CD31 for the measurement of capillary density. Digital images were taken under 200x total magnification and analyzed by Axiovision software (Zeiss, Thornwood, NY, USA). For each muscle, six nonoverlapping regions of the triceps surae complex were analyzed (approximately 600 fibers/muscle sections).

RNA isolation and quantitative PCR

Total RNA was isolated from mechanically homogenized muscle in 1 ml of Trizol reagent. All centrifuge steps were performed at 12 000 g at 4 °C. Homogenized samples were centrifuged for 15 min, and the resulting top aqueous layer was transferred to a microcentrifuge tube containing 200 μL of chloroform. After a 15-min incubation period, the samples were centrifuged for 15 min. The top aqueous layer was added to 0.5 mL of isopropyl alcohol, mixed well, and centrifuged for 10 min. The RNA pellet was washed with 75% ethanol, air-dried, and resuspended in DEPC water for RT–PCR analysis. cDNA was made using a QuantiTect Reverse Transcription Kit (Qiagen, Valencia, CA, USA). The resulting cDNA was analyzed by quantitative PCR with unlabeled primers in SYBR Green PCR Master Mix (Applied Biosystems, Foster City, CA, USA) for 40 cycles at an annealing temperature of 59 °C. Each sample was run in triplicate. The following primer sequences were used in this study: MuRF1: 5′-GCTGGTGGAAAACATCATTGACAT-3′ and 5′-CATCG GGTGGCTGCCTTT-3′; MAFbx: 5′-GACTGGACTTCTCGACTGCC-3′ and 5′-TCAGGGATGTGAGCTGTGAC-3′; FOXO1: 5′-AAGAGCGTGCCCTAC TTCAA-3′ and 5′-TGCTGTGAAGGGACAGATTG-3′; eMHC: 5′-ACT TCA CCT CTA GCC GGA TG-3′ and 5′-ATT GTC AGG AGC CAC GAA A-3′; Rpl39: 5′-CAAAATCGCCCTATTCCTCA-3′ and 5′-AGACCCAGCTTCGTT CTCCT-3′.

Western blots

Muscle tissue was homogenized in sucrose lysis buffer. 10–20 μg was prepared in Laemmli sample loading buffer, separated by SDS-PAGE, and transferred to a polyvinylidene difluoride membrane. Equal loading was verified by Ponceau stain. The membranes were incubated overnight at 4 °C in 1X Tris-buffered saline–Tween (TBST) with the appropriate antibodies: Following three rinses in 1x TBST, membranes were incubated with corresponding secondary antibodies (Vector and Pierce). After three additional washes, membranes were visualized with chemiluminescent substrate (Millipore, Temecula, CA, USA). Protein Oxidation was measured using the OxiSelect™Protein Carbonyl Immunoblot Kit according to the manufacturer's instructions, except a 1:2000 dilution was made for the anti-DNP antibody instead of the recommended 1:1000 (Cell Biolabs, San Diego, CA, USA). A total of 10 μg of protein was loaded onto a 10% SDS-PAGE gel. Immobilon Western Chemiluminescent HRP substrate (Millipore) was used to detect the oxidized proteins. Image acquisition and band quantification were performed using the ChemiDoc™ MP System and Image Lab 4.1 software (Bio-Rad, Hercules, CA, USA). The following antibodies were used in this study: actin (0.5 ng mL^{-1}, Sigma), antipolyubiquitin (1:2000, FK1, Biomol), PA28α (1:1000, Biomol), β1i (1:1000, Biomol; Biomol-Enzo Life Sciences, Farmingdale, NY, USA), RPT6 and β5i (1:1000, commercially made and affinity purified by 21st Century Biochemicals), β5 (1:1250, Biomol), PSMA6 (1:1000, Epitomics, Burlingame, CA, USA), RPT1 (1:1000, Enzo Life Sciences, Farmingdale, NY, USA), HIF-1α (1:500, Santa Cruz), total S6K1 (1:1000, Santa Cruz, Santa Cruz, CA, USA), and BiP (1:1000, BD Biosciences, San Jose, CA, USA). CHOP (1:1000), PDI (1:1000), phospho-S6K1 (1:1000), phospho- and total AKT (1:1000), Bcl2 (1:1000), and B-actin (1:5000) were obtained from Cell Signaling.

ELISA-based measurements of polyubiquitinated proteins

Muscle homogenate (1 μg) was incubated overnight at 4 °C to optimize binding to the bottom of 96-well ELISA plates (Santa Cruz Biotech). Samples were incubated in blocking buffer (1% BSA/1x PBST), rinsed three times in 1x PBS, and incubated with antipolyubiquitin (1:2000, FK1, Biomol). Following three rinses in 1x PBST, secondary antibody conjugated to horseradish peroxidase (HRP) was added. TMB substrate was added to initiate a color change reaction proportional to HRP activity, and 2.5M sulfuric acid was added to stop the reaction. The quantification of polyubiquitinated proteins was measured spectrophotometrically at a wavelength of 450 nm. Absorbance values for wells containing 1% BSA were used as background controls. The specificity of the polyubiquitin antibody was validated with purified ubiquitin and a penta-ubiquitinated chain (Biomol) (Hwee *et al.*, 2011).

Proteasome activity

20S and 26S proteasome activity assays were performed as previously described (Gomes *et al.*, 2006). All assays were carried out in a total

volume of 100 μL in 96-well opaque plates. The final composition of the 20S assay buffer was 250 mM HEPES, 5 mM EDTA, and 0.03% SDS (pH 7.5). The final composition of the 26S assay buffer was 50 mM Tris, 1 mM EDTA, 150 mM NaCl, 5 mM $MgCl_2$, 50 μM ATP, and 0.5 mM dithiothreitol (pH 7.5). Powdered muscle was homogenized by a Dounce tissue grinder in 26S buffer. Samples were centrifuged for 30 min at 12 000 g. The resulting supernatant was used to assess proteasome activity. The individual caspase-like (β1), trypsin-like (β2), and chymotrypsin-like (β5) activities of the 20S and 26S proteasome were measured by calculating the difference between fluorescence units recorded with or without the specific inhibitors in the reaction medium. β1 was initiated by the addition of 10 μL of 1 mM Z-Leu-Leu-Glu-7-AMC (Peptides Int); β2 by 10 μL of 1 mM Boc-Leu-Ser-Thr-Arg-7-amido-4-methylcoumarin (Bachem); and β5 by 10 μL of 1 mM of succinyl-Leu-Leu-Val-Tyr-7-amido-4-methylcoumarin (LLVY-AMC) (Bachem). The β1, β2, and β5 subunit assays were carried out in the absence and presence of their respective inhibitors: 40 nM Z-Pro-Nle-Asp-al (Biomol), 40 μM epoxomicin, and 10 μM epoxomicin (Peptides Int.). These substrates were cleaved by the proteasome subunits releasing free AMC. Released AMC was measured using a Fluoroskan Ascent fluorometer (Thermo Electron, Waltham, MA, USA) at an excitation wavelength of 390 nm and an emission wavelength of 460 nm. Fluorescence was measured at 15-min intervals for 2 h. All assays were linear in this range, and each sample was assayed in quadruplicate.

Caspase-3 activity

Caspase-3 activity was measured fluorometrically in 96-well opaque plates. 50 μg of protein supernatant was added to an assay buffer containing 100 mM HEPES, 0.2% CHAPS, 200 mM NaCl, 2 mM EDTA, 20% glycerol (v/v), and fresh 20 mM dithiothreitol (pH 7.4). Caspase activation was initiated by the addition of 100 μM of caspase-3 substrate Ac-DEVD-AMC (Biomol). This substrate is cleaved by caspase-3, releasing free AMC which is detected fluorometrically by a Fluoroskan Ascent fluorometer (Thermo Electron) at an excitation wavelength of 390 nm and an emission wavelength of 460 nm. Caspase-3 activity was measured by calculating the difference between fluorescence units recorded with or without caspase inhibitor 10 μM Ac-DEVD-CHO (Biomol). Fluorescence was measured at 15-minute intervals for 2 h. All assays were linear in this range, and each sample was assayed in quadruplicate. Activity is expressed as mean ± SEM.

Calpain activity

Calpain activity was measured fluorometrically in 96-well opaque plates. 50 μg of protein supernatant was added to an assay buffer containing 50 mM Tris, 1 mM EDTA, 10 mM $CaCl_2$, 150 mM NaCl, and fresh 0.5 mM dithiothreitol (pH 7.4). Calpain activity was initiated by the addition of 200 μM of substrate LLVY-AMC (Bachem). This substrate is cleaved by calpain, releasing free AMC which is detected fluorometrically by a Fluoroskan Ascent fluorometer (Thermo Electron) at an excitation wavelength of 390 nm and an emission wavelength of 460 nm. Calpain activity was measured by calculating the difference between fluorescence units recorded in the presence and absence of 50 μM calpain inhibitor IV (Calbiochem). Fluorescence was measured at 15-min intervals for 2 h. All assays were linear in this range, and each sample was assayed in quadruplicate. Activity is expressed as mean ± SEM. This assay measures both calpain I and II activities.

Statistical analysis

Two-way ANOVA was performed to access the effect of age and genotype using Sigma Stat 3.1 (Systat Software, San Jose, CA, USA). Tukey's post hoc analysis was used to determine differences when interactions existed. A one-way ANOVA was performed to determine significance in cases where only one independent variable (age or genotype) was being examined. Results are expressed as mean ± SEM, with significance set as $P < 0.05$.

Acknowledgments

This research was supported by grants from the Muscular Dystrophy Association and the National Institutes of Health (DK75801). Partial support for DTH was provided by HHMI-IMBS56006769 and T32HL086350 training fellowships.

References

Altun M, Besche HC, Overkleeft HS, Piccirillo R, Edelmann MJ, Kessler BM, Goldberg AL, Ulfhake B (2010) Muscle wasting in aged, sarcopenic rats is associated with enhanced activity of the ubiquitin proteasome pathway. *J. Biol. Chem.* **285**, 39597–39608.

Anvar SY, t Hoen PA, Venema A, van der Sluijs B, van Engelen B, Snoeck M, Vissing J, Trollet C, Dickson G, Chartier A, Simonelig M, van Ommen GJ, vander Maarel SM, Raz V (2011) Deregulation of the ubiquitin-proteasome system is the predominant molecular pathology in OPMD animal models and patients. *Skelet. Muscle* **1**, 15.

Baehr LM, Furlow JD, Bodine SC (2011) Muscle sparing in Muscle RING Finger 1 null mice: response to synthetic glucocorticoids. *J. Physiol.* **589**, 4759–4776.

Bodine SC, Latres E, Baumhueter S, Lai VK, Nunez L, Clarke BA, Poueymirou WT, Panaro FJ, Na E, Dharmarajan K, Pan ZQ, Valenzuela DM, DeChiara TM, Stitt TN, Yancopoulos GD, Glass DJ (2001) Identification of ubiquitin ligases required for skeletal muscle atrophy. *Science* **294**, 1704–1708.

Clavel S, Coldefy AS, Kurkdjian E, Salles J, Margaritis I, Derijard B (2006) Atrophy-related ubiquitin ligases, atrogin-1 and MuRF1 are up-regulated in aged rat Tibialis Anterior muscle. *Mech. Ageing Dev.* **127**, 794–801.

Combaret L, Dardevet D, Bechet D, Taillandier D, Mosoni L, Attaix D (2009) Skeletal muscle proteolysis in aging. *Curr Opin Clin Nutr Metab Care* **12**, 37–41.

Deldicque L, Bertrand L, Patton A, Francaux M, Baar K (2011) ER stress induces anabolic resistance in muscle cells through PKB-induced blockade of mTORC1. *PLoS ONE* **6**, e20993.

Du J, Wang X, Miereles C, Bailey JL, Debigare R, Zheng B, Price SR, Mitch WE (2004) Activation of caspase-3 is an initial step triggering accelerated muscle proteolysis in catabolic conditions. *J. Clin. Investig.* **113**, 115–123.

Ferrington DA, Husom AD, Thompson LV (2005) Altered proteasome structure, function, and oxidation in aged muscle. *FASEB J.* **19**, 644–646.

Fu HY, Minamino T, Tsukamoto O, Sawada T, Asai M, Kato H, Asano Y, Fujita M, Takashima S, Hori M, Kitakaze M (2008) Overexpression of endoplasmic reticulum-resident chaperone attenuates cardiomyocyte death induced by proteasome inhibition. *Cardiovasc. Res.* **79**, 600–610.

Gaugler M, Brown A, Merrell E, Disanto-Rose M, Rathmacher JA, Reynolds TH 4th (2011) PKB signaling and atrogene expression in skeletal muscle of aged mice. *J. Appl. Physiol.* **111**, 192–199.

Gomes AV, Zong C, Edmondson RD, Li X, Stefani E, Zhang J, Jones RC, Thyparambil S, Wang GW, Qiao X, Bardag-Gorce F, Ping P (2006) Mapping the murine cardiac 26S proteasome complexes. *Circ. Res.* **99**, 362–371.

Gomes AV, Waddell DS, Siu R, Stein M, Dewey S, Furlow JD, Bodine SC (2012) Upregulation of proteasome activity in muscle RING finger 1-null mice following denervation. *FASEB J.* **26**, 2986–2999.

Haas KF, Woodruff E 3rd, Broadie K (2007) Proteasome function is required to maintain muscle cellular architecture. *Biol. Cell* **99**, 615–626.

Hepple RT, Qin M, Nakamoto H, Goto S (2008) Caloric restriction optimizes the proteasome pathway with aging in rat plantaris muscle: implications for sarcopenia. *Am. J. Physiol. Regul. Integr. Comp. Physiol.* **295**, R1231–R1237.

Husom AD, Peters EA, Kolling EA, Fugere NA, Thompson LV, Ferrington DA (2004) Altered proteasome function and subunit composition in aged muscle. *Arch. Biochem. Biophys.* **421**, 67–76.

Hwee DT, Bodine SC (2009) Age-related deficit in load-induced skeletal muscle growth. *J. Gerontol. A Biol. Sci. Med. Sci.* **64**, 618–628.

Hwee DT, Gomes AV, Bodine SC (2011) Cardiac proteasome activity in Muscle Ring Finger-1 null mice at rest and following synthetic glucocorticoid treatment. *Am. J. Physiol. Endocrinol. Metab.* **301**, E967–E977.

Janssen I, Heymsfield SB, Ross R (2002) Low relative skeletal muscle mass (sarcopenia) in older persons is associated with functional impairment and physical disability. *J. Am. Geriatr. Soc.* **50**, 889–896.

Koga H, Kaushik S, Cuervo AM (2011) Protein homeostasis and aging: the importance of exquisite quality control. *Ageing Res. Rev.* **10**, 205–215.

Labeit S, Kohl CH, Witt CC, Labeit D, Jung J, Granzier H (2010) Modulation of muscle atrophy, fatigue and MLC phosphorylation by MuRF1 as indicated by hindlimb suspension studies on MuRF1-KO mice. *J. Biomed. Biotechnol.* **2010**, 693741.

Lee CK, Klopp RG, Weindruch R, Prolla TA (1999) Gene expression profile of aging and its retardation by caloric restriction. *Science* **285**, 1390–1393.

Leger B, Derave W, De Bock K, Hespel P, Russell AP (2008) Human sarcopenia reveals an increase in SOCS-3 and myostatin and a reduced efficiency of Akt phosphorylation. *Rejuvenation Res.* **11**, 163–175B.

Low P (2011) The role of ubiquitin-proteasome system in ageing. *Gen. Comp. Endocrinol.* **172**, 39–43.

Min JN, Whaley RA, Sharpless NE, Lockyer P, Portbury AL, Patterson C (2008) CHIP deficiency decreases longevity, with accelerated aging phenotypes accompanied by altered protein quality control. *Mol. Cell. Biol.* **28**, 4018–4025.

Nelson WB, Smuder AJ, Hudson MB, Talbert EE, Powers SK (2012) Cross-talk between the calpain and caspase-3 proteolytic systems in the diaphragm during prolonged mechanical ventilation. *Crit. Care Med.* **40**, 1857–1863.

Patterson C, Ike C, Willis PW 4th, Stouffer GA, Willis MS (2007) The bitter end: the ubiquitin-proteasome system and cardiac dysfunction. *Circulation* **115**, 1456–1463.

Riederer BM, Leuba G, Vernay A, Riederer IM (2011) The role of the ubiquitin proteasome system in Alzheimer's disease. *Exp. Biol. Med. (Maywood)* **236**, 268–276.

Rudolf R, Bogomolovas J, Strack S, Choi KR, Khan MM, Wagner A, Brohm K, Hanashima A, Gasch A, Labeit D, Labeit S (2012) Regulation of nicotinic acetylcholine receptor turnover by MuRF1 connects muscle activity to endo/lysosomal and atrophy pathways. *Age (Dordr)*. doi:10.1007/s11357-012-9468-9.

Sitnick M, Bodine SC, Rutledge JC (2009) Chronic high fat feeding attenuates load-induced hypertrophy in mice. *J. Physiol.* **587**, 5753–5765.

Strucksberg KH, Tangavelou K, Schroder R, Clemen CS (2010) Proteasomal activity in skeletal muscle: a matter of assay design, muscle type, and age. *Anal. Biochem.* **399**, 225–229.

Thomson DM, Gordon SE (2006) Impaired overload-induced muscle growth is associated with diminished translational signalling in aged rat fast-twitch skeletal muscle. *J. Physiol.* **574**, 291–305.

Tomaru U, Takahashi S, Ishizu A, Miyatake Y, Gohda A, Suzuki S, Ono A, Ohara J, Baba T, Murata S, Tanaka K, Kasahara M (2012) Decreased proteasomal activity causes age-related phenotypes and promotes the development of metabolic abnormalities. *Am. J. Pathol.* **180**, 963–972.

Valdez G, Tapia JC, Kang H, Clemenson GD Jr, Gage FH, Lichtman JW, Sanes JR (2010) Attenuation of age-related changes in mouse neuromuscular synapses by caloric restriction and exercise. *Proc. Natl Acad. Sci. USA* **107**, 14863–14868.

Vernace VA, Schmidt-Glenewinkel T, Figueiredo-Pereira ME (2007) Aging and regulated protein degradation: who has the UPPer hand? *Aging Cell* **6**, 599–606.

Wang XH, Zhang L, Mitch WE, LeDoux JM, Hu J, Du J (2010) Caspase-3 cleaves specific 19 S proteasome subunits in skeletal muscle stimulating proteasome activity. *J. Biol. Chem.* **285**, 21249–21257.

Whidden MA, Smuder AJ, Wu M, Hudson MB, Nelson WB, Powers SK (2010) Oxidative stress is required for mechanical ventilation-induced protease activation in the diaphragm. *J. Appl. Physiol.* **108**, 1376–1382.

Wong E, Cuervo AM (2010) Integration of clearance mechanisms: the proteasome and autophagy. *Cold Spring Harb. Perspect. Biol.* **2**, a006734.

Zhang K, Kaufman RJ (2006) Protein folding in the endoplasmic reticulum and the unfolded protein response. *Handb. Exp. Pharmacol.* **172**, 69–91.

Supporting Information

Additional Supporting Information may be found in the online version of this article at the publisher's web-site.

Fig. S1 Force-Frequency relationship and fiber cross-sectional areas of the gastrocnemius muscle of WT and MuRF1 KO mice at 18 and 24 months of age.

Fig S2 Capillary density in the gastrocnemius muscle of 18 and 24m old WT and MuRF1 KO mice.

Fig. S3 Expression of 19S and 20S proteasome subunits in young and old WT and MuRF1 KO mice.

Fig. S4 Quantification of the phosphorylation and total protein levels of Akt and S6K1 in the plantaris muscle of old WT and MuRF1 KO mice following functional overload.

Table S1 Muscle isometric twitch properties of WT and MuRF1 KO mice.